ACS OMEGA

Open Access

http://pubs.acs.org/journal/acsodf

Article

Robust Supercooled Liquid Formation Enables All-Optical Switching Between Liquid and Solid Phases of TEMPO

Jacob B. Rodriguez, Kevin Lam, Touhid Bin Anwar, and Christopher J. Bardeen*

Cite This: *ACS Omega* 2024, 9, 11266−11272

Read Online

ACCESS | Metrics & More | Article Recommendations | Supporting Information

ABSTRACT: Organic molecules that undergo supercooling can provide the basis for novel stimuli-responsive materials, but the number of such compounds is limited. Results in this paper show that the stable organic radical 2,2,6,6-tetramethyl-1-piperidine-1-oxyl (TEMPO) can form a stable supercooled liquid (SCL). Upon melting and cooling back to room temperature, the TEMPO SCL can persist for months, even after mild physical agitation. Its high vapor pressure can enable crystal growth at remote locations within the sample container over the course of days. Optical, electron paramagnetic resonance, and birefringence measurements show no evidence of new chemical species or partially ordered phases in the supercooled liquid. TEMPO's free radical character permits absorption of visible light that can drive photothermal melting to form the SCL, while a single nanosecond light pulse can initiate recrystallization of the SCL at some later time. This capability enables all-optical switching between the solid and the SCL phases. The physical origin of TEMPO's remarkable stability as an SCL remains an open question, but these results suggest that organic radicals comprise a new class of molecules that can form SCLs with potentially useful properties.

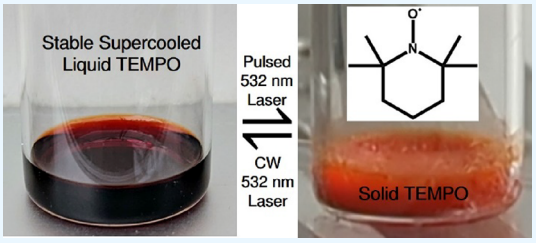

INTRODUCTION

Solid glasses[1] and crystals[2,3] composed of small organic molecules have attracted attention as functional materials. Recently, molecular liquids have begun to receive interest as functional materials as well.[4−6] There are two ways in which a molecule can exist in the liquid phase at room temperature. First, it can exist as a thermodynamically stable liquid with its melting temperature T_m < 25 °C. Alternatively, it can exist as a supercooled liquid (SCL) when its T_m > 25 °C. Supercooling occurs when a liquid is cooled below its T_m but is unable to reach the thermodynamic minimum solid-state due to kinetic barriers.[7,8] This metastable liquid can undergo sudden crystallization when a perturbation is applied. The liquid-to-solid transformation usually involves dramatic changes in optical properties (scattering, luminescence output) as well as physical properties such as viscosity and compressibility. Although supercooling can complicate the search for thermodynamically stable functional molecular liquids[9] and on-demand energy release from heat storage media,[10,11] it also presents opportunities to create new types of stimuli-responsive functional materials. Examples include mechanically induced crystallization of an SCL that can be used for rewritable inks,[12−15] as well as phase change materials that store heat that can be released when solidification is induced.[16] The ability of SCLs to undergo solidification when exposed to a specific stimulus is key to their utility. Ideally, an SCL should be kinetically stable in the absence of this stimulus, so it can be stored indefinitely until solidification is desired.

While studying the magnetic properties of the stable free radical 2,2,6,6-tetramethyl-1-piperidine-1-oxyl (TEMPO) (structure shown in Scheme 1, melting point T_m = 38°), we found that it remained liquid after cooling back to room temperature. We were surprised that this commonly used, commercially available molecule could persist as a stable SCL over months, comparable to the best reported lifetimes of synthetic organic SCLs.[17,18] Spectroscopic studies revealed no indication of significant differences between TEMPO molecules isolated in solution and those in the neat solid and liquid phases.

Scheme 1. Chemical Structure of 2,2,6,6-Tetramethyl-1-piperidinyloxy (TEMPO)

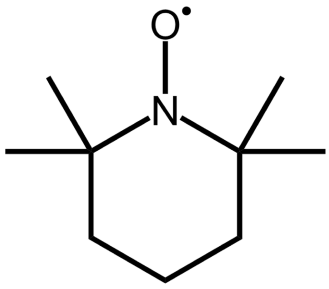

Received: September 5, 2023
Revised: January 17, 2024
Accepted: January 25, 2024
Published: February 26, 2024

The radical nature of TEMPO gives rise to an absorption feature that extends past 600 nm. We took advantage of this absorption to demonstrate laser-induced melting to form an SCL followed by impulsive laser heating to induce crystallization. There have been multiple demonstrations of optical control of solid → liquid phase transitions (melting)[19−26] as well as liquid → solid transitions.[27,28] The results in this paper demonstrate that optical control of an SCL solid → liquid → solid phase change sequence is also possible. Furthermore, spin active liquids like the TEMPO SCL are fundamentally interesting from a materials standpoint.[29] The physical origin of TEMPO's remarkable stability as an SCL remains an open question, but our results suggest that small molecule free radicals may be worth considering as a design motif for this class of materials.

EXPERIMENTAL SECTION

Sample Preparation. 2,2,6,6-Tetramethyl-1-piperidine-1-oxyl (TEMPO, Sigma-Aldrich, 98% purity) and 4-hydroxy-2,2,6,6-tetramethyl-1-piperidine-1-oxyl (TEMPOL, Tokyo Chemical Industry) were used as received. To prepare a typical SCL sample, 1.2 ± 0.20 g of TEMPO was loaded into a 20 mL glass scintillation vial with a polyethylene-lined screw cap (VWR, part number 66022−128). Lower mass samples could also be prepared in 2 mL autosampler vials (Fisher, part number 03−391−8), NMR tubes, plastic vials, and 1 mm diameter capillary tubing. The glass containers were either used as received or cleaned by using different solvents (acetone, MeOH, and HCl). Glass vials were also cleaned by soaking them in room temperature Piranha solution (a 3:1 v/v mixture of concentrated sulfuric acid and 30% hydrogen peroxide) for 40 min. Thermal melting was achieved in a Barnstead Thermolyne 1400 furnace set to 41 °C, and samples were immediately removed from the oven and allowed to cool undisturbed on a benchtop to reach room temperature.

UV−Visible Spectroscopy (UV−vis). All UV−vis measurements were performed by using a Cary 60 UV−vis Spectrophotometer. TEMPO solutions in chloroform were analyzed in a 1 cm path length quartz cuvette, while the TEMPO SCL absorption was measured using a 1 mm path length quartz cuvette. For solid TEMPO measurements, a few drops of liquid TEMPO were cast onto a microscope slide (Eisco 1 in. × 3 in., 1.1 mm thick) under a coverslip (Fisherbrand Microscope Cover Glass 25 × 25 mm). Solidification was induced by gently tapping the slide after cooling to room temperature.

Electron Paramagnetic Resonance (EPR). EPR measurements were conducted using a Bruker Magnettech ESR5000. Samples were run with a center field of 338 mT, sweep width of 50 mT, modulation of 0.2, frequency of 100 kHz, and power of 10.0 mW.

Differential Scanning Calorimetry (DSC). DSC scans were performed by using a Netzsch 214 Polyma differential scanning calorimeter. Measurements were done with variable heating and cooling rates, ranging from 0.2 to 5.0 °C min^{-1}, over a total range of 5−60 °C. After melting and cooling, the samples were held at 20 °C for 30 min to confirm that no solidification occurred in the metal sample holder.

Optical Melting and Solidification. Optical melting was achieved by exposing 200 mg of solid TEMPO to a 532 nm continuous wave (cw) laser for 5 min at a power of 2 W. After the sample melted, supercooling was confirmed by observing the liquid for up to 1 h at room temperature. Solidification of the SCL was triggered by a single 532 nm pulse, with an energy of 270 mJ and a duration of 5 ns, generated by using a Continuum Surelight SLII-10 laser.

Powder X-ray Diffraction (PXRD). TEMPO was crushed into a fine powder using a mortar and pestle. PXRD was performed by using a Panalytical Empyrean Series 2 diffractometer with CuKα radiation (λ = 1.5418 Å, 45 kV/40 mA power). The following slit sizes were used: incident divergence (1/2°), incident antiscatter (1°), and diffracted antiscatter (P8.0). The sample stage was set to spin with a revolution time of 2 s and step size of 0.0131°.

Polarized Optical Microscopy. A few drops of liquid TEMPO were cast onto a microscope slide (Eisco 1 in. x 3 in., 1.1 mm-thick) under a coverslip (Fisherbrand Microscope Cover Glass 25 × 25 mm). The sample was allowed to cool to room temperature before capturing unpolarized and polarized images using a Leica MC120 HD 2.5 Megapixel Microscope Camera. Solidification of the SCL TEMPO was induced by gently tapping the microscope slide, and images of the solid sample were subsequently acquired.

Viscosity Measurements. To assess the viscosity of SCL TEMPO in comparison to melted TEMPO, a 3.18 mm OD ball bearing was dropped into a 17.78 mm long NMR tube filled with TEMPO. Videos were recorded at 60 frames per second (0.016 s accuracy) using a Google Pixel 6 phone. For liquid TEMPO, NMR tubes were heated to 45 °C followed by immediate use. In the case of SCL TEMPO, the filled tubes were heated to 45 °C and allowed to cool before the experiment. Water (viscosity = 0.89 cP at 25 °C) was used as a standard.

RESULTS AND DISCUSSION

When the heating curve of TEMPO was measured in a standard DSC experiment, a pronounced endothermic peak at 38 °C was observed, corresponding to the reported melting transition (Figure 1). Integration of this peak allowed us to calculate an

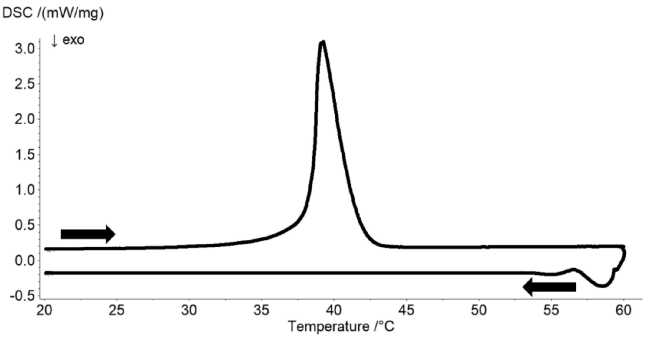

Figure 1. DSC thermogram for TEMPO with a heating/cooling rate of 5 °C min^{-1} illustrating an endothermic melting peak at 38 °C upon heating but no exothermic peak upon cooling, which is an indication of supercooling behavior.

enthalpy of fusion of 13.8 ± 0.4 kJ/mol (88.3 ± 2.5 kJ/kg). This value is comparable to that of benzene[30] but well below that of typical phase change materials used for thermal storage.[31] After the temperature ramp was reversed and the sample was cooled, no corresponding exothermic peak due to resolidification was observed in the DSC curve. Varying the heating and cooling rates from 0.2 to 5.0 °C min^{-1} had no effect on the shape of the DSC curves (Supporting Information, Figure S1). Subsequent heating of the SCL did not lead to crystallization, suggesting that the TEMPO SCL was relatively stable against temperature perturbations.

https://doi.org/10.1021/acsomega.3c06717
ACS Omega 2024, 9, 11266−11272

The DSC results were confirmed by visible inspection of TEMPO samples that were melted in an oven and then cooled to room temperature. The presence of the liquid phase could be easily determined by eye, since crystallization of the SCL led to a large increase in the sample's light scattering. Polarized light microscopy gave no indication of any residual birefringence in the SCL (Supporting Information, Figure S2). PXRD measurements showed sharp peaks from the solid that could be assigned to orthorhombic and monoclinic polymorphs, but the SCL exhibited only a single very broad peak at $2\theta = 15.3°$ (Supporting Information, Figures S3−S5). The broad peak is characteristic of organic molecular liquids and reflects the nearest neighbor scattering in the liquid.[32−34] No sharp peaks were observed that would indicate the presence of a partially ordered or liquid crystal phase. Using the falling ball method and water as a standard, we measured the viscosity of the SCL to be 1.2 cP at 25 °C. This value was approximately 10% greater than the value measured for the melt at 44 °C. The increased viscosity of the room temperature SCL is consistent with the expected change in liquid viscosity due to the lower temperature, which is in the range for a structurally similar liquid like methylcyclohexane (Supporting Information).[35] None of these measurements provided evidence of significant structural differences between the SCL and the pure liquid in a high temperature melt. It is possible, however, that more sophisticated rheology measurements could provide evidence for the existence of cooperative regions or longer relaxation times in the SCL.[36]

Supercooling was observed for TEMPO as received (reported as 98% pure) and for TEMPO purified by sublimation, suggesting that supercooling was not an artifact of chemical impurities. Furthermore, SCL formation was observed in a wide variety of glass containers, including 20 mL vials, NMR tubes, and 1 mm diameter glass capillaries. Within a set of 20 mL vials containing ∼1 g of TEMPO, the longevity of the SCL depended on which vial was used. Some vials would support the SCL for only a few hours, while others could maintain the SCL for weeks or months. If one of these long-lived vials was emptied and refilled with fresh TEMPO, the long-lived SCL was still observed, whereas a short-lived vial was never observed to support a long-lived SCL. We suspected that this variation might be due to chemical impurities or solid residue inside the vial. However, the use of various cleaning protocols, ranging from acetone rinsing to Piranha acid cleaning, had no measurable effect on the ability of a specific vial to support a long-lived SCL. Based on these observations, we hypothesize that the solidification of the SCL in a stationary container is induced by the presence of microscale structural defects on the container walls, rather than by chemical impurities or intrinsic nucleation events within the melt itself.

Some TEMPO SCL samples persisted for up to 6 months with no sign of crystallization, even after swirling or gentle shaking (Figure 2, and Supporting Information, Video S1). In order to check whether these samples could still crystallize, we used two methods. First, if the cap was removed and the vial left open to the air for several minutes, solidification typically occurred within 10 min. We suspect that the impact of microscopic dust particles from the ambient air induced crystallization. If the SCL was vented through a small opening that prevented dust entry, it would survive for hours while slowly evaporating. The second method involved direct mechanical perturbation by dipping a pipet tip into the SCL and withdrawing some liquid, which induced crystallization within a few seconds (Supporting Information, Video S2). Note that simply contacting the SCL with a clean pipet tip was not sufficient to induce immediate crystallization. A full characterization of the mechanical conditions under which crystallization can be induced would be desirable but is left for future work.

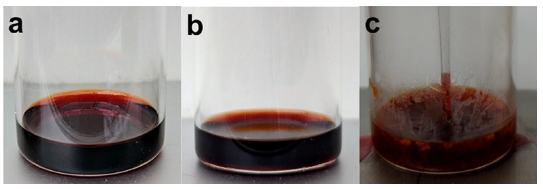

Figure 2. Observation of a TEMPO SCL sample at the following time points: (a) immediately after removal from oven, (b) after 5 months sitting undisturbed, and (c) after nucleation is induced by insertion of a glass pipet tip.

For the long-lived (>1 week) samples, the most common mode of crystallization in a closed vial involved growth of a seed crystal separated from the liquid. Over the course of days, a TEMPO crystal would nucleate and grow on the walls or cap of the vial. As the crystal extended from the nucleation point, sometimes up to several centimeters in length, parts of it could break off and drop into the SCL. These fragments acted as seed crystals for solidification. In some cases, the crystal would actually grow all the way down to the SCL to seed crystallization (Figure 3). The stability of the TEMPO SCL, combined with its higher vapor pressure, enabled crystal growth via evaporation of the SCL and recondensation of the vapor as a solid at a distant location within the container. This type of secondary crystal growth was never observed for a solid TEMPO sample held under the same conditions (Supporting Information, Figure S6). Sublimation from the solid was apparently negligible over the same time frame. This observation is consistent with previous studies on water[37] and organic molecules[38] that have shown the SCLs have significantly higher vapor pressures than their solids. New crystal growth could be initiated at a specific location within a few hours by placing a small amount of solid TEMPO in a capillary in the desired location above the SCL, although the resulting crystal needles typically grew in random directions from the seed (Supporting Information, Figure S7). These observations show that the TEMPO SCL can be used as a reservoir to supply molecules for crystal growth at a remote location in a sealed system.

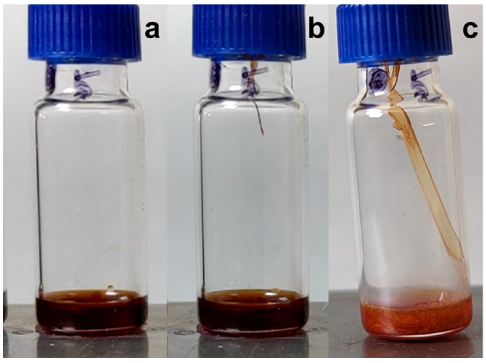

Figure 3. Remote crystal growth from a TEMPO SCL observed at different time intervals: (a) SCL after 1 h, (b) SCL after 12 days with incipient crystal needle growing from top, and (c) after 16 days the crystal needle reaches the SCL and induces crystallization.

To actively induce crystallization of the SCL in a closed system, we utilized the visible absorption of the nitroxide radical

https://doi.org/10.1021/acsomega.3c06717
ACS Omega 2024, 9, 11266−11272

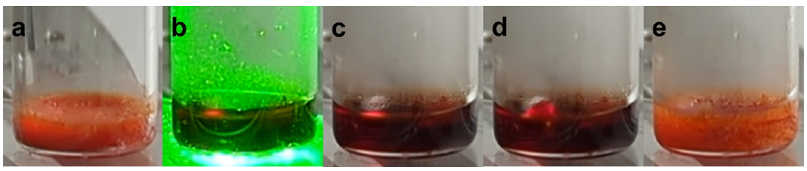

Figure 4. Optically induced melting of TEMPO and solidification of SCL TEMPO in a 2 mL glass vial: (a) initial solid state, (b) melting process using a 2W cw 532 nm laser, (c) stable SCL formed after laser melting, (d) impact of the single nanosecond 532 nm laser pulse laser indicated by the splash mark formed toward the left of the vial, and (e) solid TEMPO formed after the single nanosecond pulse impacts the SCL.

that provides a way to heat the sample by using light. We previously used TEMPO as a photothermal agent for wax melting,[39] but in this work, we used a 532 nm laser to melt solid TEMPO itself. Figure 4 shows a 100 mg mass of TEMPO being melted by a cw 532 nm laser beam. Using 2 W of laser power, the TEMPO melted completely within 2 min. The laser melted TEMPO persisted as an SCL for at least 1 h after the laser was turned off. As observed for thermal heating in an oven, solidification could not be induced using the cw laser to slowly reheat the SCL. In order to trigger crystallization, we used a pulsed 532 nm laser to impulsively heat the sample (Supporting Information, Video S3). A single 5 ns, 270 mJ laser pulse could vaporize part of the liquid, and the resultant bursting gas bubble provided enough mechanical perturbation to trigger solidification, which occurred within 200 ms of laser impact (Figure 4). We suspected that the laser melting might have been incomplete, leaving some residual crystals on the sides of the vial that could act as seeds when the laser pulse perturbed the SCL. To eliminate this possibility, we confirmed that the same laser pulse could also trigger the recrystallization of an SCL generated by oven melting, where no residual seed crystals could exist. We also confirmed that laser melting and recrystallization did not affect a sample's ability to form an SCL afterward, which suggests that the 532 nm laser exposure did not generate new chemical species that changed the SCL properties.

To fully characterize the laser-induced solid → liquid → solid process, we would ideally measure the wavelength dependence for both melting and solidification, but we were limited by the availability of suitable laser sources to 532 nm. Given the strong overlap of 532 nm with the TEMPO absorption, we assume that direct absorption of the laser light and photothermal vaporization provide the mechanical perturbation to trigger crystallization. Similar mechanical perturbation of an SCL using ultrasonication[40] or laser cavitation[41] have both been shown to be capable of triggering crystallization. These mechanical methods are distinct from other laser-induced crystallization phenomena that rely on high fields to align and trap molecules in solution,[28,42] or on nonlinear laser breakdown to produce chemical defects in the liquid that act as nucleation sites.[43] The optically induced thermal-mechanical method used here to induce a solid → liquid → solid cyclic transformation complements earlier work that relied on photochemistry to accomplish a similar cycle.[27]

The chemical origin of TEMPO's ability to form SCLs is not obvious. One possible explanation for the stability of the SCL would be the formation of a new chemical species in the liquid phase that inhibits crystallization. UV−vis absorption measurements on TEMPO in dilute solution, in the solid-state, and in the SCL phase (Figure 5) all showed the same broad, featureless peak due to the nitroxide radical n → π^* transition,[44] albeit shifted to slightly longer wavelengths in the solid and SCL. The absorption red-shift and broadening are consistent with the higher dielectric and polarizability of the neat TEMPO samples

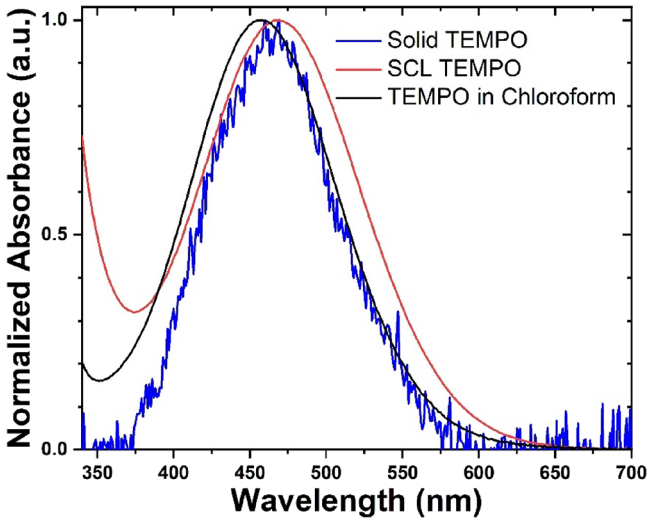

Figure 5. UV−vis absorption spectra of solid TEMPO (blue), TEMPO SCL (red), and dilute TEMPO in a chloroform solution (black) at 293 K.

as compared to liquid $CHCl_3$.[45] The EPR lineshapes of the solid and the SCL were quite similar except for some additional broadening in the solid (Figure 6a). We confirmed that isolated TEMPO molecules in liquid solution exhibited the expected hyperfine splitting due to the spin = 1 nitrogen atom (Figure 6b) that collapsed to a single derivative feature in the neat solid and liquid due to enhanced exchange interactions.[46] Previous work has shown that nitroxide radicals can form head-to-head dimers or oligomers in solution with distinct EPR signatures,[47,48] but these splittings would likely be swamped by the broadening due to rapid exchange in the dense liquid. However, the similar EPR intensities for solid and SCL samples suggested that the spin densities of both phases were within 10% of each other; therefore, there was no indication of extensive spin pairing. Neither UV−vis nor EPR measurements provided clear evidence of new chemical species that could explain the SCL stability.

If extraneous chemical species do not stabilize the liquid, then the molecular structure itself must play a role. In general, the use of strategic alkyl substitution to decrease molecular symmetry has been successfully used to inhibit crystal growth,[9,49] although exceptions to this rule have also been found.[50] The low ΔH_{fus} of TEMPO indicates that there is not a strong thermodynamic driving force for crystal formation. If the intermolecular interactions are enhanced by adding a hydrogen bonding group, we expect that there will be a stronger driving force for crystallization and no SCL formation. This hypothesis was tested using 4-hydroxy-2,2,6,6-tetramethyl-1-piperidine-1-oxyl (TEMPOL), in which an OH group is added to the six-membered ring opposite the NO group. This derivative crystallized immediately after being removed from the oven

https://doi.org/10.1021/acsomega.3c06717
ACS Omega 2024, 9, 11266−11272

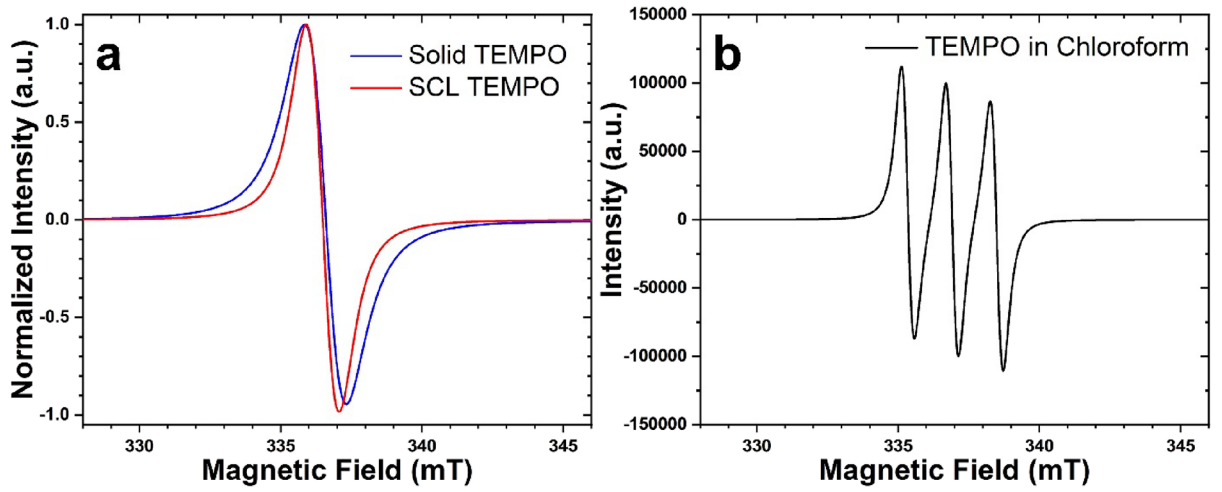

Figure 6. EPR spectra of (a) solid TEMPO (blue) and TEMPO SCL (red) and (b) dilute TEMPO in chloroform (black) solution at 293 K.

with no sign of supercooling, suggesting that the presence of a strong directing group can overcome the thermodynamic factors that give rise to stable SCL for TEMPO.

Finally, we examined whether TEMPO's solid-state structure could provide clues for the SCL stability. TEMPO exhibits three different crystal phases,[51] two of which have been fully characterized by single crystal X-ray diffraction. In the monoclinic form, the TEMPO molecules align themselves in head-to-tail rows with the nitroxide substituents pointing in the same direction.[52,53] The orthorhombic form exhibits very different packing without well-defined layers or orientational ordering.[54] PXRD measurements showed that solid TEMPO is composed of a mixture of monoclinic and orthorhombic forms. The starting crystal mixture had no effect on formation of the SCL. Resolidification from both the melt and SCL regenerated a monoclinic/orthorhombic mixture, although the relative weighting of the two forms can change (Supporting Information, Figure S5). Recent work has suggested that solid-state polymorphism can translate to polyamorphism in supercooled liquids.[55] Because sustained crystal growth requires the formation of a nucleus above a critical size,[56] one possible explanation for the stability of the TEMPO SCL is that very different microscopic arrangements coexist within the liquid and frustrate largescale crystal growth of either phase. Additional measurements that quantitatively characterize the physical properties of the SCL (vapor pressure, rheology, nucleation kinetics) will be required to evaluate this speculative mechanism.

CONCLUSIONS

In this paper, we characterized the remarkably robust SCL phase of the stable free radical TEMPO. Upon melting and cooling back to room temperature, the SCL can persist for months even after mild physical agitation. The SCL's high vapor pressure can enable crystal growth at remote locations within the sample container. TEMPO's free radical character permits absorption of visible light for melting, while a nanosecond pulse of light can induce recrystallization from the SCL. The capability of cycling between solid and liquid phases using only light as a stimulus may be useful for applications like controllable adhesion or modifying light transmission properties. Although the exact mechanism of the SCL stability is a subject for future investigation, the discovery of TEMPO's supercooling abilities opens up a new class of materials for potential applications as SCLs.

ASSOCIATED CONTENT

Supporting Information

The Supporting Information is available free of charge at https://pubs.acs.org/doi/10.1021/acsomega.3c06717.

Figure S1: DSC thermograms of SCL TEMPO; Figure S2: polarized light microscopy of SCL and solid TEMPO; Figure S3: powder X-ray diffraction measurements of different TEMPO phases; Figure S4: simulated powder X-ray diffraction measurements from the CCDC database of the orthorhombic (black) and monoclinic (red) polymorphs of TEMPO; Figure S5: powder X-ray diffraction measurement of resolidified TEMPO SCL; Supporting Information eq 1: temperature-dependent viscosity m of a liquid calculation; Figure S6: no separate crystal growth is observed in the solid TEMPO sample under identical conditions to SCL; Figure S7: crystal growth at the tip of a TEMPO-filled capillary tube suspended over an SCL sample; Figure S8: crystal growth of TEMPO by SCL evaporation observed at different time intervals; Scheme S1: chemical structure of 4-hydroxy-2,2,6,6-tetramethyl-1-piperidinyloxyl (TEMPOL); Figure S9: fitting for the solid TEMPO absorption plot in Figure 5 (PDF)

Video S1: physical perturbation via swirling did not induce solidification of the TEMPO SCL − 1.0× speed (MP4)

Video S2: induced nucleation by the insertion of a glass pipet tip − 2.5× speed (MP4)

Video S3: optically induced solidification of SCL TEMPO in a 2 mL glass vial using a single nanosecond 532 nm laser pulse − 1.0× speed (MP4)

AUTHOR INFORMATION

Corresponding Author

Christopher J. Bardeen − *Materials Science and Engineering, Department of Chemistry, and Department of Chemical and Environmental Engineering, University of California, Riverside, Riverside, California 92521, United States;* orcid.org/0000-0002-5755-9476; Email: christopher.bardeen@ucr.edu

https://doi.org/10.1021/acsomega.3c06717
ACS Omega 2024, 9, 11266−11272

Authors

Jacob B. Rodriguez − *Materials Science and Engineering, University of California, Riverside, Riverside, California 92521, United States;* orcid.org/0009-0000-6097-6011

Kevin Lam − *Department of Chemistry, University of California, Riverside, Riverside, California 92521, United States;* orcid.org/0009-0007-6606-8170

Touhid Bin Anwar − *Department of Chemical and Environmental Engineering, University of California, Riverside, Riverside, California 92521, United States*

Complete contact information is available at: https://pubs.acs.org/10.1021/acsomega.3c06717

Notes

The authors declare no competing financial interest.

■ ACKNOWLEDGMENTS

This work was supported by the Office of Naval Research through the MURI on Photomechanical Material Systems (ONR N00014-18-1-2624).

■ REFERENCES

(1) Ediger, M. D.; de Pablo, J.; Yu, L. Anisotropic Vapor-Deposited Glasses: Hybrid Organic Solids. *Acc. Chem. Res.* **2019**, *52*, 407−414.

(2) Podzorov, V. Organic single crystals: Addressing the fundamentals of organic electronics. *MRS Bull.* **2013**, *38*, 15−24.

(3) Naumov, P.; Chizhik, S.; Panda, M. K.; Nath, N. K.; Boldyreva, E. Mechanically Responsive Molecular Crystals. *Chem. Rev.* **2015**, *115*, 12440−12490.

(4) Santhosh Babu, S.; Nakanishi, T. Nonvolatile functional molecular liquids. *Chem. Commun.* **2013**, *49*, 9373−9382.

(5) Ghosh, A.; Nakanishi, T. Frontiers of solvent-free functional molecular liquids. *Chem. Commun.* **2017**, *53*, 10344−10357.

(6) Tateyama, A.; Nakanishi, T. Responsive molecular liquid materials. *Respons. Mater.* **2023**, *1*, No. e20230001.

(7) Ediger, M. D.; Angell, C. A.; Nagel, S. R. Supercooled Liquids and Glasses. *J. Phys. Chem.* **1996**, *100*, 13200−13212.

(8) Cavagna, A. Supercooled liquids for pedestrians. *Phys. Rep.* **2009**, *476*, 51−124.

(9) Lu, F.; Jang, K.; Osica, I.; Hagiwara, K.; Yoshizawa, M.; Ishii, M.; Chino, Y.; Ohta, K.; Ludwichowska, K.; Kurzydłowski, K. J.; Ishihara, S.; Nakanishi, T. Supercooling of functional alkyl-p molecular liquids. *Chem. Sci.* **2018**, *9*, 6774−6778.

(10) Ryu, H. W.; Woo, S. W.; Shin, B. C.; Kim, S. D. Prevention of supercooling and stabilization of inorganic salt hydrates as latent heat storage materials. *Sol. Energy Mater. Sol. Cells* **1992**, *27*, 161−172.

(11) Lane, G. A. Phase change materials for energy storage nucleation to prevent supercooling. *Sol. Energy Mater. Sol. Cells* **1992**, *27*, 135−160.

(12) Chung, K.; Kwon, M. S.; Leung, B. M.; Wong-Foy, A. G.; Kim, M. S.; Kim, J.; Takayama, S.; Gierschner, J.; Matzger, A. J.; Kim, J. Shear-Triggered Crystallization and Light Emission of a Thermally Stable Organic Supercooled Liquid. *ACS Cent. Sci.* **2015**, *1*, 94−102.

(13) Hariharan, P. S.; Moon, D.; Anthony, S. P. Crystallization-induced reversible fluorescence switching of alkyl chain length dependent thermally stable supercooled organic fluorescent liquids. *CrystEngComm* **2017**, *19*, 6489−6497.

(14) Butler, T.; Wang, F.; Daly, M. L.; DeRosa, C. A.; Dickie, D. A.; Sabat, M.; Fraser, C. L. Supercooled Liquid β-Diketones with Mechanoresponsive Emission. *J. Phys. Chem. C* **2019**, *123*, 25788−25800.

(15) Sato, Y.; Mutoh, Y.; Morishita, S.; Tsurumachi, N.; Isoda, K. Stimulus-Responsive Supercooled π-Conjugated Liquid and Its Application in Rewritable Media. *J. Phys. Chem. Lett.* **2021**, *12*, 3014−3018.

(16) Kutlu, C.; Su, Y.; Lyu, Q.; Riffat, S. Thermal management of using crystallization-controllable supercooled PCM in space heating applications for different heating profiles in the UK. *Renew. Energy* **2023**, *206*, 848−857.

(17) Yin, Z.; Zhao, Y.; Wan, S.; Yang, J.; Shi, Z.; Peng, S. X.; Chen, M. Z.; Xie, T. Y.; Zeng, T. W.; Yamamuro, O.; Nirei, M.; Akiba, H.; Zhang, Y. B.; Yu, H. B.; Zeng, M. H. Synergistic Stimulation of Metal−Organic Frameworks for Stable Super-cooled Liquid and Quenched Glass. *J. Am. Chem. Soc.* **2022**, *144*, 13021−13025.

(18) Komura, M.; Ogawa, T.; Tani, Y. Room-temperature phosphorescence of a supercooled liquid: kinetic stabilisation by desymmetrisation. *Chem. Sci.* **2021**, *12*, 14363−14368.

(19) Norikane, Y.; Hirai, Y.; Yoshida, M. Photoinduced isothermal phase transitions of liquid-crystalline macrocyclic azobenzenes. *Chem. Commun.* **2011**, *47*, 1770−1772.

(20) Hoshino, M.; Uchida, E.; Norikane, Y.; Azumi, R.; Nozawa, S.; Tomita, A.; Sato, T.; Adachi, S.-i.; Koshihara, S.-y. Crystal Melting by Light: X-ray Crystal Structure Analysis of an Azo Crystal Showing Photoinduced Crystal-Melt Transition. *J. Am. Chem. Soc.* **2014**, *136*, 9158−9164.

(21) Ishiba, K.; Morikawa, M.-a.; Chikara, C.; Yamada, T.; Iwase, K.; Kawakita, M.; Kimizuka, N. Photoliquefiable Ionic Crystals: A Phase Crossover Approach for Photon Energy Storage Materials with Functional Multiplicity. *Angew. Chem., Int. Ed.* **2015**, *54*, 1532−1536.

(22) Saito, S.; Nobusue, S.; Tsuzaka, E.; Yuan, C.; Mori, C.; Hara, M.; Seki, T.; Camacho, C.; Irle, S.; Yamaguchi, S. Light-Melt Adhesive Based on Dynamic Carbon Frameworks in a Columnar Liquid-Crystal Phase. *Nat. Commun.* **2016**, *7*, 12094/12091−12097.

(23) Xu, W.-C.; Sun, S.; Wu, S. Photoinduced Reversible Solid-to-Liquid Transitions for Photoswitchable Materials. *Angew. Chem., Int. Ed.* **2019**, *58*, 9712−9740.

(24) Gerkman, M. A.; Gibson, R. S. L.; Calbo, J.; Shi, Y.; Fuchter, M. J.; Han, G. G. D. Arylazopyrazoles for Long-Term Thermal Energy Storage and Optically Triggered Heat Release below 0 °C. *J. Am. Chem. Soc.* **2020**, *142*, 8688−8695.

(25) Kuenstler, A. S.; Clark, K. D.; Read de Alaniz, J.; Hayward, R. C. Reversible Actuation via Photoisomerization-Induced Melting of a Semicrystalline Poly(Azobenzene). *ACS Macro Lett.* **2020**, *9*, 902−909.

(26) Komura, M.; Sotome, H.; Miyasaka, H.; Ogawa, T.; Tani, Y. Photoinduced crystal melting with luminescence evolution based on conformational isomerisation. *Chem. Sci.* **2023**, *14*, 5302−5308.

(27) Akiyama, H.; Kanazawa, S.; Okuyama, Y.; Yoshida, M.; Kihara, H.; Nagai, H.; Norikane, Y.; Azumi, R. Photochemically Reversible Liquefaction and Solidification of Multiazobenzene Sugar-Alcohol Derivatives and Application to Reworkable Adhesives. *ACS Appl. Mater. Interfaces* **2014**, *6*, 7933−7941.

(28) Alexander, A. J.; Camp, P. J. Non-photochemical laser-induced nucleation. *J. Chem. Phys.* **2019**, *150*, No. 040901.

(29) Zielinska, A.; Takai, A.; Sakurai, H.; Saeki, A.; Leonowicz, M.; Nakanishi, T. A Spin-Active, Electrochromic, Solvent-Free Molecular Liquid Based on Double-Decker Lutetium Phthalocyanine Bearing Long Branched Alkyl Chains. *Chem. - Asian J.* **2018**, *13*, 770−774.

(30) Xu, W.; Zhu, R.; Tian, Y.; Li, H.; Li, H. Fusion Curves and Enthalpy and Internal Energy Changes of Benzene, Nitrobenzene, Bromobenzene, and Chlorobenzene at Pressures up to 3500 MPa. *J. Chem. Eng. Data* **2007**, *52*, 1975−1978.

(31) Patil, J. R.; Mahanwar, P. A.; Sundaramoorthy, E.; Mundhe, G. S. A review of the thermal storage of phase change material, morphology, synthesis methods, characterization, and applications of micro-encapsulated phase change material. *J. Polym. Eng.* **2023**, *43*, 354−375.

(32) Stewart, G. W. X-Ray Diffraction in Liquid Normal Paraffins. *Phys. Rev.* **1928**, *31*, 174−179.

(33) Stewart, G. W. Diffraction of X-Rays in Liquids: Benzene, Cyclohexane and Certain of Their Derivatives. *Phys. Rev.* **1929**, *33*, 889−899.

(34) Tohji, K.; Murata, Y. X-Ray Diffraction Study of the Melting of Benzene. *Jpn. J. Appl. Phys.* **1982**, *21*, 1199−1204.

(35) Reid, R. C.; Prausnitz, J. M.; Poling, B. E. *The Properties of Gases and Liquids*. 4 ed.; McGraw-Hill: New York, 1987.

(36) Sen, S.; Zhu, W.; Aitken, B. G. Behavior of a supercooled chalcogenide liquid in the non-Newtonian regime under steady vs. oscillatory shear. *J. Chem. Phys.* **2017**, *147*, No. 034503.
(37) Murphy, D. M.; Koop, T. Review of the vapour pressures of ice and supercooled water for atmospheric applications. *Q. J. R. Meteorol. Soc.* **2005**, *131*, 1539−1565.
(38) Lei, Y. D.; Chankalal, R.; Chan, A.; Wania, F. Supercooled Liquid Vapor Pressures of the Polycyclic Aromatic Hydrocarbons. *J. Chem. Eng. Data* **2002**, *47*, 801−806.
(39) Lui, B. F.; Bardeen, C. J. Using Small Molecule Absorbers to Create a Photothermal Wax Motor. *Small* **2022**, *18*, No. 2105356.
(40) Inada, T.; Zhang, X.; Yabe, A.; Kozawa, Y. Active control of phase change from supercooled water to ice by ultrasonic vibration 1. Control of freezing temperature. *Int. J. Heat Mass Transfer* **2001**, *44*, 4523−4531.
(41) Beaupere, N.; Soupremanien, U.; Zalewski, L. Nucleation triggering methods in supercooled phase change materials (PCM), a review. *Thermochim. Acta* **2018**, *670*, 184−201.
(42) Garetz, B. A.; Matic, J.; Myerson, A. S. Polarization Switching of Crystal Structure in the Nonphotochemical Light-Induced Nucleation of Supersaturated Aqueous Glycine Solution. *Phys. Rev. Lett.* **2002**, *89*, No. 175501.
(43) Lindinger, B.; Mettin, R.; Chow, R.; Lauterborn, W. Ice Crystallization Induced by Optical Breakdown. *Phys. Rev. Lett.* **2007**, *99*, No. 045701.
(44) Falbo, E.; Fusè, M.; Lazzari, F.; Mancini, G.; Barone, V. Integration of Quantum Chemistry, Statistical Mechanics, and Artificial Intelligence for Computational Spectroscopy: The UV−Vis Spectrum of TEMPO Radical in Different Solvents. *J. Chem. Theory Comput.* **2022**, *18*, 6203−6216.
(45) Bardeen, C. J. The Structure and Dynamics of Molecular Excitons. *Annu. Rev. Phys. Chem.* **2014**, *65*, 127−148.
(46) Capiomont, A.; Chion, B.; Lajzerowicz-Bonneteau, J.; Lemaire, H. Interpretation and utilization for crystal stucture determination of ESR spectra of single crystals of nitroxide free radicals. *J. Chem. Phys.* **1974**, *60*, 2530−2535.
(47) Kooser, R. G. Nitroxide Spin Label Dimer Pairing: A Cautionary Note. *Macromolecules* **1987**, *20*, 435−436.
(48) Kanzaki, Y.; Shiomi, D.; Sato, K.; Takui, T. Biradical Paradox Revisited Quantitatively: A Theoretical Model for Self-Associated Biradical Molecules as Antiferromagnetically Exchange Coupled Spin Chains in Solution. *J. Phys. Chem. B* **2012**, *116*, 1053−1059.
(49) Zheng, X.; Nagura, K.; Takaya, T.; Hashi, K.; Nakanishi, T. Quest for a Rational Molecular Design of Alkyl-Distyrylbenzene Liquid by Substitution Pattern Modulation. *Chem. - Eur. J.* **2023**, *29*, No. e202203775.
(50) Lu, F.; Shinohara, A.; Kawamura, I.; Saeki, A.; Takaya, T.; Iwata, K.; Nakanishi, T. Room-Temperature Alkyl-Diphenylpyrene Liquefication by Molecular Desymmetrization. *Helv. Chim. Acta* **2023**, *106*, No. e202300050.
(51) Bordeaux, D.; Bornarel, J.; Capiomont, A.; Lajzerowicz-Bonneteau, J.; Lajzerowicz, J.; Legrand, J. F. New Ferroelastic-Ferroelectric Compound: Tanane. *Phys. Rev. Lett.* **1973**, *31*, 314−317.
(52) Stefan, S.; Belaj, F.; Madl, T.; Pietschnig, R. A Radical Approach to Hydroxylaminotrichlorosilanes: Synthesis, Reactivity, and Crystal Structure of TEMPO-$SiCl_3$ (TEMPO = 2,2,6,6-Tetramethylpiperidine-N-oxyl). *Eur. J. Inorg. Chem.* **2010**, *2010*, 289−297.
(53) Ranjan, S.; Takamizawa, S. Characterization of Organo-ferroelasticity in a TEMPO Crystal. *Cryst. Growth Des.* **2022**, *22*, 585−589.
(54) Yonekuta, Y.; Oyaizu, K.; Nishide, H. Structural Implication of Oxoammonium Cations for Reversible Organic One-electron Redox Reaction to Nitroxide Radicals. *Chem. Lett.* **2007**, *36*, 866−867.
(55) Walton, F.; Bolling, J.; Farrell, A.; MacEwen, J.; Syme, C. D.; Jiménez, M. G.; Senn, H. M.; Wilson, C.; Cinque, G.; Wynne, K. Polyamorphism Mirrors Polymorphism in the Liquid−Liquid Transition of a Molecular Liquid. *J. Am. Chem. Soc.* **2020**, *142*, 7591−7597.
(56) Chung, K.; Yang, D. S.; Kim, J., Functional Organic Supercooled Liquids. In *Functional Organic Liquids*, Nakanishi, T., Ed. Weinheim, Germany: New York, 2019.

https://doi.org/10.1021/acsomega.3c06717
ACS Omega 2024, 9, 11266−11272